Alloy phase formation in nanometer-sized particles in the In-Sn system

J. G. Lee,[1] H. Mori,[1] and H. Yasuda[2]
[1]*Research Center for Ultra-High Voltage Electron Microscopy, Osaka University, Yamadaoka, Suita, Osaka 565-0871, Japan*
[2]*Department of Mechanical Engineering, Kobe University, Rokkodai, Nada, Kobe 657-8501, Japan*
(Received 6 September 2001; revised manuscript received 10 December 2001; published 27 March 2002)

Alloy phase formation in the In-Sn binary system has been studied as a function of the particle size by *in situ* transmission electron microscopy at room temperature. In approximately 16-nm-sized particles, alloy phases formed were essentially the same as for those in bulk material. However, in particles less than approximately 10 nm in size, the formation of a liquid phase, which is not an equilibrium phase in bulk at room temperature, was confirmed. The formation of the liquid phase can be ascribed to the large suppression of the eutectic temperature associated with the size reduction.

DOI: 10.1103/PhysRevB.65.132106 PACS number(s): 64.70.−p

In recent years, much attention has been focused on small particles in the size range from a few to several nanometers. This is because these nanometer-sized particles often exhibit structures and properties that are different from those of the corresponding bulk materials.[1,2] For example, with regard to structures, it is well known that the stable structure of indium undergoes a change from bct for bulk to fcc when the size of particles is reduced to several nanometers.[3] Also, it is well established that such phase-transition temperatures as the melting point are significantly reduced with decreasing size of particles.[4–6] All these examples are in relation to the phase transition in nanometer-sized *pure* substances, and to the authors' knowledge, studies on the alloy phase formation in nanometer-sized particles in the binary systems are quite limited,[7–10] although an abundance of work has been carried out on the phase transformations in binary nanocrystals.[11,12]

Recent remarkable progress in transmission electron microscopy enables us to study not only the structure but also the chemical composition of nanometer-sized target materials, and with the use of the technique it now becomes possible to examine the phase stability of isolated nanometer-sized alloy particles as a function of temperature (T), composition (C), and size (d) of the system. This situation would open a wide research field on the structure stability of nanometer-sized condensed matter in two- (or multi-) component systems. In fact, quite recently it was discovered by this technique that a thermally stable amorphous phase, which to our best knowledge has never been observed in bulk materials, does appear in isolated Au-Sn alloy particles when the size of particle is smaller than about 6 nm.[10] The formation of the thermally stable amorphous phase is ascribed to the large suppression of the eutectic temperature (T_{eu}) induced by the size reduction.[10] Namely, due to the large suppression, a situation in which room temperature (RT) where observations were carried out, lies below the glass transition temperature (T_g) but above T_{eu} (that is, $T_g > \mathrm{RT} > T_{\mathrm{eu}}$) has been achieved in the 6-nm-sized Au-Sn alloy particles.[10] This observation is of some significance in that it revealed the following: in nanometer-sized alloy particles it becomes possible that T_g lies above T_{eu} and at the relative position among RT (where observations are performed), T_g and T_{eu} play an important role in understanding the phase stability in nanometer-sized alloy particles. One of other possible relative positions among the three temperatures is the case where they lie in the order $\mathrm{RT} > T_g > T_{\mathrm{eu}}$ and in this case it is predicted that a crystalline-to-liquid ($C \rightarrow L$) transition will be observed at RT by simply adding (appropriate) solute atoms onto nanometer-sized crystalline particles of a pure substance (crystalline particles composed of solvent atoms only). The present paper reports on the direct observation of such a $C \rightarrow L$ transition, found in particles in the In-Sn system.

Preparation of nanometer-sized indium particles and subsequent vapor deposition of tin onto indium particles were carried out using a double-source evaporator installed in the specimen chamber of a Hitachi H-800 200-kV transmission electron microscope (TEM). The evaporator consisted of two spiral-shaped tungsten filaments. The distance between the filaments and a supporting film (substrate) for particles was approximately 100 nm. An amorphous carbon film was used as the supporting film, and was mounted on a molybdenum grid. Using this evaporator, indium was first evaporated from one filament onto the supporting film kept at ambient temperature, and nanometer-sized indium particles were produced on the film. Next, tin was evaporated from the other filament onto the same film kept at ambient temperature. Alloy phase formation in the nanometer-sized particles associated with tin deposition was studied by TEM. The microscope was equipped with a turbomolecular pumping system to achieve a base pressure of around 5×10^{-5} Pa in the specimen chamber. The electron flux used was approximately 1.5×10^{20} $\mathrm{em}^{-2}\mathrm{s}^{-1}$.

In order to study the atomistic structure of alloy phases formed, a series of alloy formation experiments were additionally carried out in a 200-kV Hitachi HF-2000 high-resolution electron microscope (HREM). The base pressure in the specimen chamber of this microscope was below 5×10^{-7} Pa. A flake of graphite was used as a supporting substrate. Prior to experiments, the flake was baked at 1073 K for 60 s to get a clean surface of graphite. After being baked, the graphite substrate was cooled to room temperature. For *in situ* HREM observation of the alloying process, a television camera and video tape recorder (VTR) system was employed. The positive were reproduced from the images recorded with the VTR system.

A typical example of alloying behavior of tin atoms into indium particles is shown in Fig. 1. Figures 1(a) and 1(a′) show a bright-field image (BFI) of as-produced indium par-

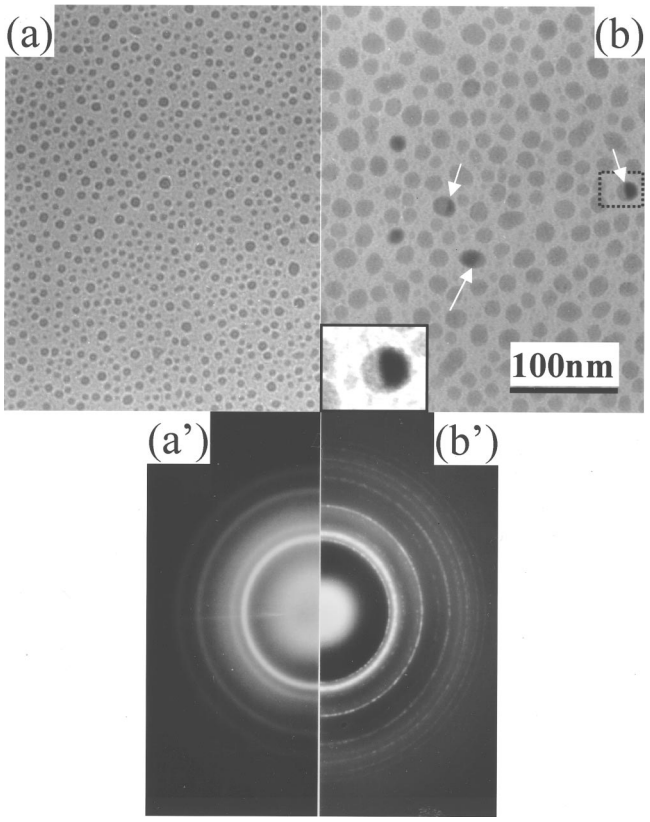

FIG. 1. Alloying behavior of tin atoms into indium particles at ambient temperature. (a) BFI of as-produced indium particles on an amorphous carbon film, and (a′) the corresponding SAED. (b) BFI of particles after depositing tin atoms, and (b′) the corresponding SAED. Inset in (b) shows an enlargement of a framed part. The mean size of particles in (b) was 16 nm in diameter. The chemical composition of the particles was evaluated to be approximately Sn-30 at % In.

ticles on a supporting film and the corresponding selected area electron-diffraction pattern (SAED), respectively. The mean diameter of indium particles is approximately 7 nm. The Debye-Scherrer rings in the SAED can consistently be indexed as those of a crystal with the face-centered-cubic (fcc) structure with a lattice constant of $a=0.471$ nm. This is essentially consistent with the results in the previous report.[3] Figures 1(b) and 1(b′) show a BFI of particles after tin deposition and the corresponding SAED, respectively. These photographs were taken immediately after tin deposition, that is, in less than 20 s after the tin-atom beam was turned off. The particle size increased from approximately 7 to 16 nm in the mean diameter, as seen from a comparison of Figs. 1(a) with 1(b). Electron probe microanalysis (EPMA) of the same sample shown in Fig. 1(b) revealed that the material on the supporting film contained, on the whole, about 70 at % Sn. One point to be noted here is the fact that a distinct hetero-interface is present in individual particles [as indicated with arrows in Fig. 1(b)]. This fact suggests that individual particles are composed of two phases. An enlargement of the SAED shown in Fig. 1(b′) is depicted in Fig. 2. As illustrated in this figure, the Debye-Scherrer rings can consistently be indexed as those of In_3Sn (which has a tetragonal structure

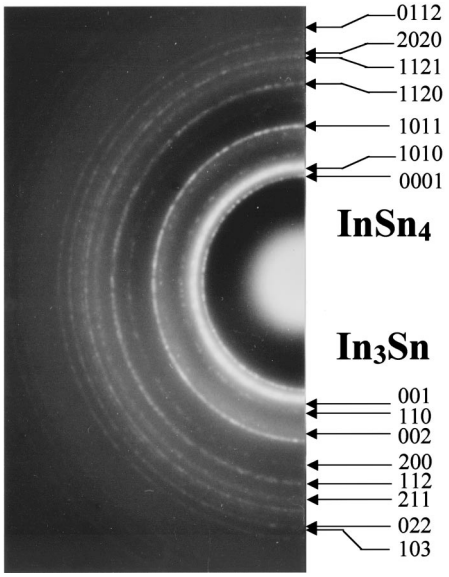

FIG. 2. An enlargement of the SAED shown in Fig. 1(b′). The Debye-Scherrer rings can be indexed as those of In_3Sn superimposed on those of $InSn_4$.

belonging to the space group $I4/mmm$ with lattice constants of $a=0.346$ and $c=0.439$ nm) superimposed on those of $InSn_4$ (which has a hexagonal structure belonging to the space group $P6/mmm$ with lattice constants of $a=0.320$ and $c=0.299$ nm). These two phases are nothing but the conjugate phases predicted from the bulk equilibrium phase diagram.[13] All these observations indicate that when tin atoms are vapor deposited onto 7-nm-sized indium particles, rapid spontaneous alloying of tin atoms into indium particles takes place and as a result a mixture of two phases, one In_3Sn and the other $InSn_4$, is developed within each particle. The formation of the two-phase mixture in individual particles is consistent with alloy phase formation expected from the phase diagram for the bulk.

The above observation is consistent with a recent result that when the size of particles is larger than about 10 nm an essentially similar phase equilibrium was observed both in particles and bulk materials in the Au-Sn binary system.[10] Therefore, it seems safe to consider that the finite-size effect on the phase stability in alloy particles is rather small when the size of particles is larger than approximately 10 nm.

An example of alloying behavior of tin atoms into relatively small indium particles is presented in Fig. 3. Figures 3(a) and 3(a′) show a BFI of as-produced indium particles and the corresponding SAED, respectively. The mean diameter of indium particles is approximately 5 nm. The Debye-Scherrer rings in the SAED can again be indexed as those of fcc pure indium. Figures 3(b) and 3(b′) show a BFI of particles after tin deposition and the corresponding SAED, respectively. The particle size has increased from approximately 5 to 10 nm in the mean diameter, as seen from a comparison of Figs. 3(a) with 3(b). It should be noted here that no interfaces are recognized in the interior of individual particles in Fig. 3(b), in contrast to the observation depicted in Fig. 1(b). In the SAED [Fig. 3(b)], halos are recognized. This fact indicates that vapor-deposited tin atoms came in

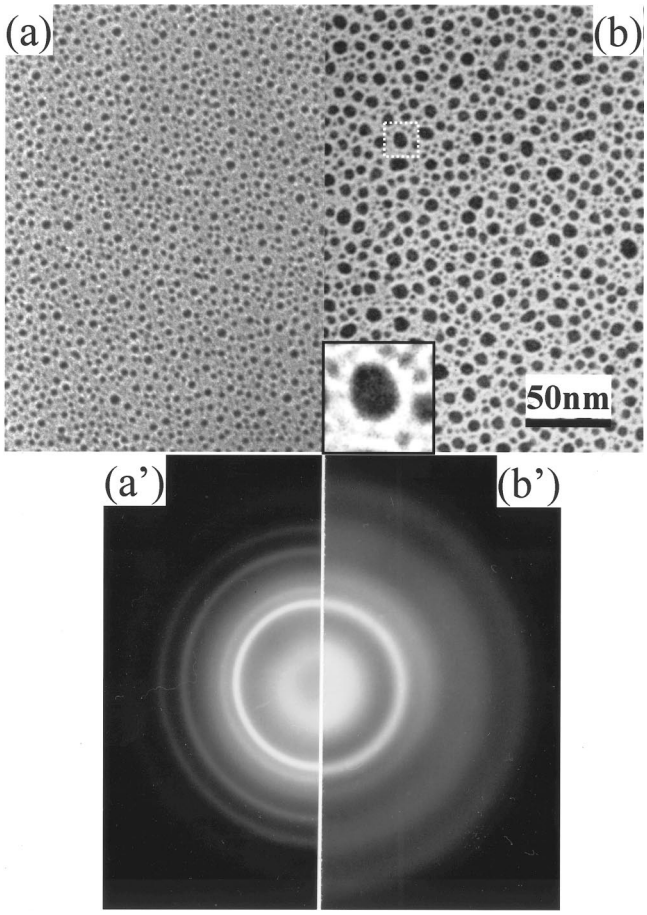

FIG. 3. Alloying behavior of tin atoms into indium particles at ambient temperature. (a) BFI of as-produced indium particles on an amorphous carbon film, and (a′) the corresponding SAED. (b) BFI of particles after depositing tin atoms, and (b′) the corresponding SAED. Inset in (b) shows an enlargement of a framed part. The mean size of particles in (b) was 10 nm in diameter. The chemical composition of the particles was evaluated to be approximately Sn-30 at % In.

contact with indium particles and dissolved quickly into the particles to form either amorphous or liquid In-Sn alloy particles. The formation of the noncrystalline phase is consistent with the observation that no interfaces are present within individual particles [Fig. 3(b)]. EPMA of the same sample shown in Fig. 3(b) revealed that the material on the supporting film contained, on the whole, about 70 at % Sn. The stable phases in the In-70 at % Sn bulk alloy at room temperature are In_3Sn and $InSn_4$, as mentioned before. Accordingly, it can be said that in In-70 at % Sn alloy particles of approximately 10 nm in the mean diameter, stable phases in the corresponding bulk material are not realized. It is of significance to investigate whether the structure of alloy particles shown in Fig. 3(b) is amorphous or liquid. However, it is difficult to solve this problem from halo rings only shown in the SAED [Fig. 3(b)]. Based upon this premise, a series of *in situ* alloying experiments was carried out in a HREM to see an atomistic structure of the noncrystalline alloy particles form.

Figure 4 is a typical sequence of the alloying process in

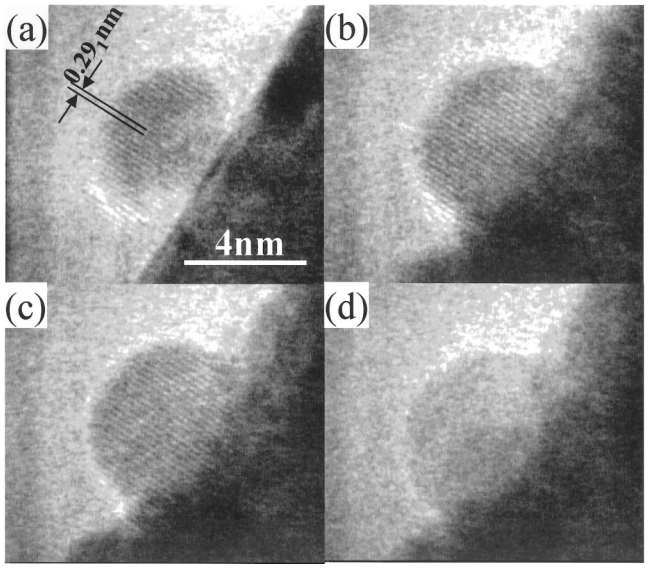

FIG. 4. *In situ* observation of alloying process of indium atoms into an approximately 4-nm-sized tin particle. A crystalline-to-liquid ($C \rightarrow L$) transition took place during deposition of indium onto the nanometer-sized tin particle kept at room temperature [compare (c) with (d)].

an approximately 4-nm-sized particle. Figure 4(a) shows an as-produced, pure tin particle on a graphite substrate. The 0.291-nm-spaced fringes seen in this particle are the (020) lattice fringes of β-Sn. The same particle after indium deposition is shown in Fig. 4(b). The particle remains a single crystal, indicating a solid solution is formed in the particle. The diameter of the particle has increased from approximately 4.0 [Fig. 4(a)] to 4.4 nm [Fig. 4(b)] during indium deposition. The indium concentration in the solid solution estimated from the size increment is approximately 25 at % In. With continued deposition of indium, the particle underwent a crystalline-to-liquid ($C \rightarrow L$) transition, as shown in Figs. 4(c) and 4(d). Namely, all the lattice fringes in the particle disappeared abruptly and there appeared only a uniform contrast typical of the liquid state [Fig. 4(d)]. The time interval between Figs. 4(c) and 4(d) is 1/15 s, indicating that the $C \rightarrow L$ transition took place very quickly.

In an attempt to confirm that such droplets as the one shown in Fig. 4(d) are not a solid amorphous phase but a liquid phase, a series of detailed HREM observations on alloy droplets was carried out. An example of the results is depicted in Fig. 5. Figure 5(a) shows an as-produced alloy particle. The particle is in a crystalline state and therefore in a state of a solid solution. The 0.292-nm-spaced fringes seen in the particle can be consistently assigned as the (020) lattice fringes of the solid solution with the β-Sn structure, while the 0.278-nm-spaced fringes can be assigned as the (101) lattice fringes. It is also noted here that the formation of facets can be clearly recognized on the surface of the particle. With continued deposition of indium, all the lattice fringes abruptly disappeared and at the same time the shape of the particle changed from faceted and polygonal to round and semispherical, as seen in Fig. 5(b). It is noteworthy that no salt-pepper contrast characteristic of a solid amorphous

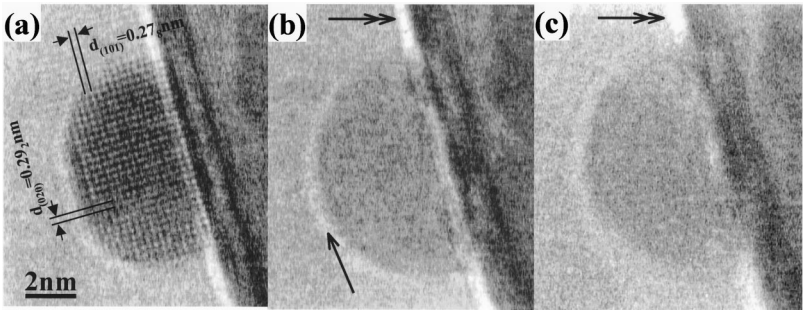

FIG. 5. A series of HREM observations on an alloy droplet. (a) HREM of an as-produced, crystalline alloy particle, (b) HREM of the same particle after a melting transition, and (c) the same field as in (b) but taken in a condition underfocused by an additional amount of 20 nm.

phase is present in the particle in Fig. 5(b). It is also worth noting in Fig. 5(b) that the Fresnel ring (arrowed) appears almost symmetrically around the particle, which indicates that astigmatism is satisfactorily corrected and therefore the absence of any contrast features does not come from such an extrinsic factor as the astigmatism but are of more intrinsic nature. Figure 5(c) shows the same field as in Fig. 5(b) but taken in a condition underfocused by an additional amount of 20 nm. The fact that Fig. 5(c) was taken in a further underfocused condition as compared to Fig. 5(b) can be confirmed from the observation that the width of the Fresnel maximum (the bright band, double arrowed) along the edge of the graphite substrate is larger in Fig. 5(c) than in Fig. 5(b). It is evident that again no salt-pepper contrast can be observed in the particle in this varied defocus condition. All these observations clearly indicate that the droplet shown in Figs. 5(b) and 5(c) is not a solid amorphous phase but a liquid phase.

The indium concentration in the liquid estimated from the size difference between the particle shown in Fig. 4(a) and that in Fig. 4(c) is approximately 30 at % In. Therefore, it can be said that the stable phase of the approximately 4-nm-sized Sn-30 at % In alloy particle at room temperature is liquid, and this is in sharp contrast with the equilibrium phase(s) in bulk materials (i.e., a two-phase mixture of In_3Sn and $InSn_4$). Through the HREM observations shown in Fig. 4, it is clarified that the structure of such alloy particles as depicted in Fig. 3(b) is not amorphous but liquid.

It is verified that a liquid phase was formed in approximately 10-nm-sized particles of an In-70 at % Sn alloy [Fig. 3(b)] and in 4-nm-sized particles of a Sn-30 at % In alloy [Fig. 4(d)] kept at room temperature, although particles of pure tin [Fig. 4(a)] and of pure indium [Fig. 3(a)] in the comparable size range remain crystalline at room temperature. The formation of the liquid phase is thought to come from a situation in which due to the suppression of T_{eu} induced by the size reduction, the three temperatures, RT, T_g, and T_{eu}, lie in an order RT$>T_g>T_{eu}$. It is interesting to note here that in case room temperature where observations were conducted lies between T_g and T_{eu}, then a crystalline-to-amorphous ($C\rightarrow A$) transition, instead of the $C\rightarrow L$ transition observed in the present work, is predicted to take place when solute atoms are deposited and that in fact such a $C\rightarrow A$ transition has been observed in 6-nm-sized particles in the Au-Sn system.[10] In this context, the present observations shown in Figs. 3–5 provide further evidence for the finite-size effect on T_{eu} and for the fact that the relative position among RT (the temperature where observations are carried out), T_g, and T_{eu} plays an important role in understanding the phase stability.

Recently it was reported by Mitome, Tanishiro, and Takayanagi[14] that the temperature rise of lead particles of 13 nm in diameter supported on a graphitized carbon substrate was within 20 K, when illuminated with 200-keV electrons at a flux of $6.3\times10^{23}-9.4\times10^{23}$ e$\cdot$m$^{-2}\cdot$s^{-1}. In the present work the flux employed is similar to these values. Therefore the temperature rise in nanometer-sized tin particles on a graphitized carbon substrate in the present work examined with the Hitachi HF-2000 HREM is estimated to be within $\sim$13 K, assuming that the temperature rise is, under a fixed-flux condition, proportional to the density ρ of the material [i.e., $\rho(\mathrm{Sn})/\rho(\mathrm{Pb})\sim0.64$].[15] Based upon this premise, it seems safe to consider that the temperature rise due to the beam heating is rather small and may not play an essential role in the alloying-induced crystalline-to-liquid transition observed in the present work.

This work was supported by the Ministry of Education, Science, and Culture under a Grant-in-Aid for Scientific Research (Grant No. 13450260).

[1] R. P. Andres *et al.*, J. Mater. Res. **4**, 704 (1987).
[2] W. P. Halperin, Rev. Mod. Phys. **58**, 533 (1986).
[3] A. Yokozeki and G. Stein, J. Appl. Phys. **49**, 2224 (1978).
[4] J. R. Sambles, Proc. R. Soc. London, Ser. A **324**, 339 (1971).
[5] Ph. Buffat and J-P. Borel, Phys. Rev. A **13**, 2287 (1976).
[6] G. L. Allen *et al.*, Thin Solid Films **144**, 297 (1986).
[7] L. S. Palatnik and B. T. Boiko, Phys. Met. Metallogr. **11**, 119 (1961).
[8] G. L. Allen and W. A. Jesser, J. Cryst. Growth **70**, 546 (1984).
[9] W. A. Jesser *et al.*, Mater. Res. Innovations **2**, 211 (1999).
[10] H. Yasuda *et al.*, Phys. Rev. B **64**, 094101 (2001).
[11] A. R. Yavari, Mater. Sci. Eng., A **179/180**, 20 (1994).
[12] R. Kikuchi and L. Q. Chen, Nanostruct. Mater. **5**, 257 (1995).
[13] *Binary Alloy Phase Diagrams*, edited by T. B. Massalski *et al.* (American Society for Metals, Metals Park, OH, 1986).
[14] M. Mitome *et al.*, Z. Phys. D: At., Mol. Clusters **12**, 45 (1989).
[15] S. B. Fisher, Radiat. Eff. **5**, 239 (1970).